ResearchGate

See discussions, stats, and author profiles for this publication at: https://www.researchgate.net/publication/224090807

Dynamic yaw and velocity control of the 6WD skid-steering mobile robot RobuROC6 using sliding mode technique

Conference Paper · November 2009

DOI: 10.1109/IROS.2009.5354373 · Source: IEEE Xplore

CITATIONS
13

READS
160

4 authors:

Eric Lucet
CEA - Atomic Energy and Alternative Energies Commission
22 PUBLICATIONS **100** CITATIONS
SEE PROFILE

Christophe Grand
The French Aerospace Lab ONERA
63 PUBLICATIONS **652** CITATIONS
SEE PROFILE

Damien Salle
Tecnalia
35 PUBLICATIONS **172** CITATIONS
SEE PROFILE

Philippe Bidaud
Pierre and Marie Curie University - Paris 6
244 PUBLICATIONS **1,784** CITATIONS
SEE PROFILE

Some of the authors of this publication are also working on these related projects:

H2020 ESPRIT Project - Coupled articulated vehicle train View project

ARMEN: Assistive robotics to maintain elderly people in natural environment View project

All content following this page was uploaded by Christophe Grand on 10 June 2014.

The user has requested enhancement of the downloaded file.

Dynamic velocity and yaw-rate control of the 6WD skid-steering mobile robot RobuROC6 using sliding mode technique

Eric Lucet [1,2], Christophe Grand [1], Damien Sallé [2] and Philippe Bidaud [1]

***Abstract*— A robust dynamic feedback controller is designed and implemented, based on the dynamic model of the six-wheel skid-steering RobuROC6 robot, performing high speed turns. The control inputs are respectively the linear velocity and the yaw angle. The main object of this paper is to elaborate a sliding mode controller, proved to be robust enough to ignore the knowledge of the forces within the wheel-soil interaction, in the presence of sliding phenomena and ground level fluctuations. Finally, a 3D simulation is performed with an accurate physical engine to evaluate the efficiency of this designed control law.**

I. INTRODUCTION

The aim of this paper is to control precisely a six wheel drive skid-steering vehicle. Nevertheless, vehicle systems are not usually easy to control because of unknowns about their behaviour and the difficulty to evaluate the forces in the wheel-soil interaction. Many interaction models developped by Bakker [3] or by Pacejka [15] try to represent the complexity of the physical phenomena by using empirical functions. However, wheel-soil interaction is still one of the great unknowns in mobile robotic systems. The dynamic of skid-steering mobile robots has been studied by Caracciolo in [5], with the use of a dynamic feedback linearization paradigm for a model-based controller that minimizes lateral skidding by imposing the longitudinal position of the instantaneous center of rotation. In [12], Kozlowski designed a new algorithm proved to have a high robustness to dynamic parameters uncertainty. Now, another strategy that uses a sliding mode controller can be investigated in order to deal with the skid phenomenon that is inherent to this kind of vehicle. This controller, developped by Utkin [19], authorizes a decoupling design procedure, a disturbance rejection, insensitivity to dynamic parameters variations, and a simple implementation. That is why this control law has been treated in many ways in the literature. In [11] and in [2] dynamic control laws are studied, but without taking into account the complex dynamical model of the vehicle. In [20] and then in [6] the dynamical model of a unicycle is studied for the design of a controller by using a nonholonomic constraint, considering a null lateral velocity. In [9], it is taken into account that in realistic case, the nonholonomic constraints are not satisfied. But the problem is addressed for a partially linearized dynamical model of a unicycle robot.

(1) Univsersity of Paris 6 - UPMC, Insitut des Systèmes Intelligents et de Robotique (CNRS - FRE 2507), France {lucet,grand,bidaud}@robot.jussieu.fr

(2) Robosoft, Technopole d'Izarbel, 64210 Bidart, France {eric.lucet,damien.salle}@robosoft.fr

Fig. 1. RobuROC6

Here, we suggest an original dynamical model based upon sliding mode control method for fast autonomous mobile robots, that controls the torques applied in the wheels. The main objective is to follow a given path with a relatively high speed by servoing the longitudinal velocity and the yaw angle. The terrains considered here are horizontal in theory and relatively smooth compared to the size of the wheels. If most of the mobile robots motion controllers found in the literature use the hypothesis of rolling without slipping, it is no longer suitable at high speed where wheel slip can not be neglected. Because of the dynamics of the vehicle and the saturation of admissible forces by the soil, the slippage reduces the robot motion stability. So a controller robust enough is needed

A 3D simulation is performed in a dynamic environment with robuBOX, a software developed by the ROBOSOFT company [1] and based on Microsoft Robotics Studio. An interaction wheel-soil model of forces designed by Szostak et al in [18], described in the fifth section, is used to permit a realistic modelling of the system behavior. We will analyze the motion control of a RobuROC6 represented Fig. 1.

It is an electric mobile robot developed by Robosoft, for exemple studied in [13], which consists of three pods steered and driven by two actuated conventional wheels on which a lateral slippage may occur. The rear and the front pods are symmetrically arranged about the central pod. They are attached to this later one by two orthogonal passive revolute joints providing a roll/pitch relative motion so as to keep the wheels on the ground to maintain traction of the pod when driving across irregular surfaces. Note that the pitch mobility can be actuated by hydraulic cylinders. Two ultrasonic sensors with a range of $3,4$ meters and two bumper sensors are located in the front and in the rear of the robot.

One inclinometer for each pod and odometric sensors are also available. A GPS and a gyroscope are needed for the control law implementation.

A controller based on a complete three dimensional dynamic model of this kind of articulated system would be difficult to investigate, especially the calcul of complex equations in a limited time if we intend to reach high velocities. That is the reason why the sliding mode controller is particulary adapted. The robustness of this controller, according to the robot dynamic model, permits to stay quite reliable in spite of the sliding phenomenon and the roll and pitch movements of the three pods, due to possible fluctuations of the ground level and of the normal contact.

This paper is organized as follows. In the second section, the system dynamical model is given. In the third section, we describe the design of the sliding mode controller. In the fourth section, the use of the Robosoft Robubox for an efficient implementation of the controller is detailed. In the last section, simulation results using this controller are presented and analyzed.

II. SYSTEM DYNAMICS MODEL

A dynamic model of a skid-steering vehicle is established in fixed frame $\mathscr{R}_0 = \{O_0, \mathbf{x}_0, \mathbf{y}_0, \mathbf{z}_0\}$. We consider $\mathscr{R} = \{G, \mathbf{x}, \mathbf{y}, \mathbf{z}_0\}$ the frame attached to the vehicle. The vehicle pose vector is given by $[x, y, \theta]^T$, where $[x, y]^T$ is the position of the center of gravity G and θ is the orientation of $\mathscr{R}$, both with respect to $\mathscr{R}_0$. The representation of the 6WD skid-steering vehicle is described Fig. 2. The absolute velocity $\left[\dot{x}, \dot{y}, \dot{\theta}\right]^T$ becomes $[u, v, r]^T$ in the local frame, linked by the relationship:

$$\begin{bmatrix} \dot{x} \\ \dot{y} \\ \dot{\theta} \end{bmatrix} = \begin{bmatrix} \cos\theta & -\sin\theta & 0 \\ \sin\theta & \cos\theta & 0 \\ 0 & 0 & 1 \end{bmatrix} \begin{bmatrix} u \\ v \\ r \end{bmatrix} \quad (1)$$

The wheel-ground interaction forces are called F_{x**} and F_{y**} for each one of the six wheels in both the longitudinal **x** and the lateral **y** directions (with f, m and r for front, middle and rear, and l and r for left and right). The dynamic model of this mechanical system can be expressed in the local frame by the following equations:

$$\begin{aligned} M(\dot{u} - rv) &= F_{xrl} + F_{xrr} + F_{xml} + F_{xmr} + F_{xfl} + F_{xfr} \quad (2) \\ M(\dot{v} + ru) &= F_{yrl} + F_{yrr} + F_{yml} + F_{ymr} + F_{yfl} + F_{yfr} \quad (3) \\ J\dot{r} &= -w_l F_{xrl} + w_r F_{xrr} - l_r F_{yrl} - l_r F_{yrr} \\ &\quad -w_l F_{xml} + w_r F_{xmr} \quad (4) \\ &\quad -w_l F_{xfl} + w_r F_{xfr} + l_f F_{yfl} + l_f F_{yfr} \end{aligned}$$

which expresses the dynamics of the main frame considered as a unique rigid body, and:

$$\begin{aligned} J_w\dot{\omega}_{fl} = \tau_{fl} - RF_{xfl} \quad ; \quad J_w\dot{\omega}_{fr} = \tau_{fr} - RF_{xfr} \quad ; \\ J_w\dot{\omega}_{ml} = \tau_{ml} - RF_{xml} \quad ; \quad J_w\dot{\omega}_{mr} = \tau_{mr} - RF_{xmr} \quad ; \quad (5) \\ J_w\dot{\omega}_{rl} = \tau_{rl} - RF_{xrl} \quad ; \quad J_w\dot{\omega}_{rr} = \tau_{rr} - RF_{xrr} \end{aligned}$$

that correspond to the wheels spin dynamics.

M is the mass of the vehicle, R the wheel radius, J the vehicle inertia on **z** axis, J_w the wheel inertia, $\dot{\omega}_{**}$ the angular acceleration of the wheels, τ_{**} the wheel torques, w_l and w_r the left and right width and l_f and l_r the front and rear length.

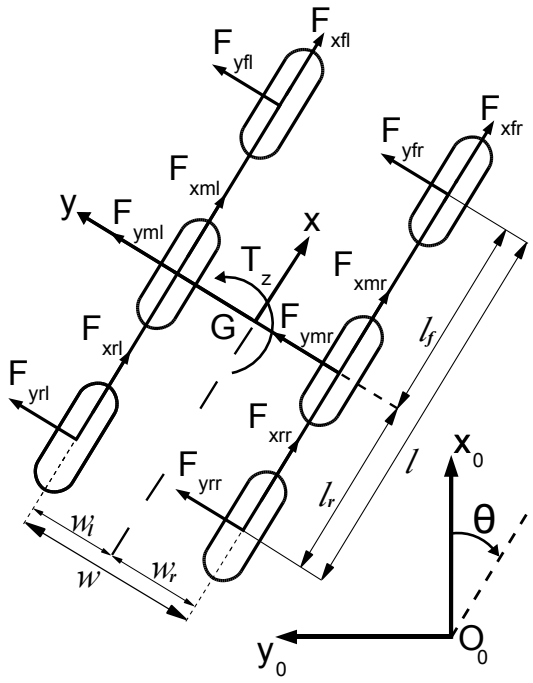

Fig. 2. System dynamics

III. CONTROLLER DESIGN

Because the lateral dynamics of the vehicle can not be controlled, we use only the dynamic equations projected along **x** and $\mathbf{z}_0$ for the decoupling design procedure.

The longitudinal velocity and the yaw angle of the vehicle are controlled by adding two inputs τ_u and τ_θ. The torque τ_u is applied equally on the six wheels of the robot, whereas the value of the torque τ_θ is of opposite sign for the right and the left wheels.

The control law architecture is depicted Fig. 3.

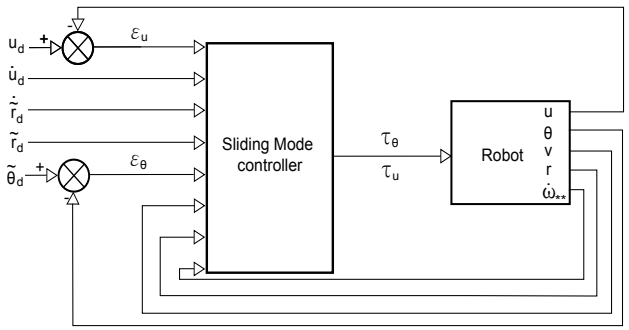

Fig. 3. Control block diagram

A. Control of the yaw angle θ

1) Design of the control law: Introducing the input τ_θ, equations (4) and (5) give us:

$$\dot{r} = \lambda \tau_\theta + \Lambda_\theta \dot{\omega} + \mathbf{D}_\theta \mathbf{F}_\mathbf{y} \tag{6}$$

with:

$$\begin{array}{lcl} \lambda & = & \frac{3}{2}\frac{w_r+w_l}{JR} \ ; \\ \Lambda_\theta & = & \frac{-J_\omega}{JR}\left[\begin{array}{cccccc} -w_l & w_r & -w_l & w_r & -w_l & w_r \end{array}\right]; \\ \dot{\omega} & = & \left[\begin{array}{cccccc} \dot{\omega}_{fl} & \dot{\omega}_{fr} & \dot{\omega}_{ml} & \dot{\omega}_{mr} & \dot{\omega}_{rl} & \dot{\omega}_{rr} \end{array}\right]^T; \\ \mathbf{D}_\theta & = & \left[\begin{array}{cccc} l_f & l_f & -l_r & -l_r \end{array}\right]; \\ \mathbf{F}_y & = & \left[\begin{array}{cccc} F_{yfl} & F_{yfr} & F_{yrl} & F_{yrr} \end{array}\right]^T. \end{array}$$

As proposed in [8], to drive the vehicle to the path, the desired yaw angle θ_d has to be modified as:

$$\tilde{\theta}_d = \theta_d + \arctan\left(\frac{d}{d_0}\right)$$

with d_0 a positive gain and d the distance to the path.

Considering $c_{d\theta}$ the control law and $n\left(\theta, r, \dot{r}, d, \dot{d}, \ddot{d}\right)$ the function of uncertainties depending on θ, r, $\dot{r}$, d, $\dot{d}$ and $\ddot{d}$ in the dynamic equations, we have the following relationship:

$$\dot{r} = c_{d\theta} - n\left(\theta, r, \dot{r}, d, \dot{d}, \ddot{d}\right) \tag{7}$$

We define the yaw angle control law as:

$$c_{d\theta} = \ddot{\tilde{r}}_d + K_p^\theta \varepsilon_\theta + K_d^\theta \dot{\varepsilon}_\theta + \sigma_\theta \tag{8}$$

with:

- $\ddot{\tilde{r}}_d$ the second derivative of $\tilde{\theta}_d$, being an anticipative term;
- $\varepsilon_\theta = \tilde{\theta}_d - \theta$ the yaw angle error;
- K_p^θ and K_d^θ two positive constants that permit to define the settling time and the overshoot of the closed-loop system;
- σ_θ the sliding mode control law.

2) Error state equation establishment: If we calculate the second derivative of ε_θ:

$$\begin{array}{lcl} \ddot{\varepsilon}_\theta & = & \ddot{\tilde{r}}_d - \dot{r} \\ & = & \ddot{\tilde{r}}_d - c_{d\theta} + n \\ & = & \ddot{\tilde{r}}_d - \left(\ddot{\tilde{r}}_d + K_p^\theta \varepsilon_\theta + K_d^\theta \dot{\varepsilon}_\theta + \sigma_\theta\right) + n \\ & = & -K_p^\theta \varepsilon_\theta - K_d^\theta \dot{\varepsilon}_\theta + (n - \sigma_\theta) \end{array} \tag{9}$$

We define the error state vector $\mathbf{x} = \begin{pmatrix} \varepsilon_\theta \\ \dot{\varepsilon}_\theta \end{pmatrix}$. So, we have the state equation:

$$\dot{\mathbf{x}} = A\mathbf{x} + B(n - \sigma_\theta) \tag{10}$$

with: $A = \begin{pmatrix} 0 & 1 \\ -K_p^\theta & -K_d^\theta \end{pmatrix}$; $B = \begin{pmatrix} 0 \\ 1 \end{pmatrix}$.

If $\sigma_\theta = 0$, the system is linear and we choose the value of K_p^θ and K_d^θ as $K_p^\theta = \omega_n^2$ and $K_d^\theta = 2\xi\omega_n$ in order to define a second order system. ω_n is the pulsation and ξ the damping factor. To define numerical values, the 5% settling time T_r is introduced: $T_r = \frac{4{,}2}{\xi\omega_n}$.

3) Stability analysis: To guarantee the stability of this closed-loop system, the problem of tracking the desired yaw angle $\tilde{\theta}_d$ can be solved by using the Lyapunov candidate function $V = \mathbf{x}^T P \mathbf{x}$, with P a positive definite symetric matrix. Based on the Lyapunov theorem ([17]), the state $\mathbf{x} = 0$ is stable only if:

$$V(0) = 0 \ ; \ \forall \mathbf{x} \neq 0 \ \ V(\mathbf{x}) > 0 \ \textit{and} \ \dot{V}(\mathbf{x}) < 0 \tag{11}$$

The first two equations are verified. We have to establish the third one. Using the equation 10, we calculate the derivative:

$$\begin{array}{lcl} \dot{V}(\mathbf{x}) & = & \dot{\mathbf{x}}^T P \mathbf{x} + \mathbf{x}^T P \dot{\mathbf{x}} \\ & = & \left(\mathbf{x}^T A^T + nB^T - \sigma_\theta B^T\right) P\mathbf{x} \\ & & + \mathbf{x}^T P (A\mathbf{x} + Bn - B\sigma_\theta) \\ & = & \mathbf{x}^T \left(A^T P + PA\right)\mathbf{x} + 2\mathbf{x}^T PB(n - \sigma_\theta) \end{array} \tag{12}$$

Then, we calculate P in order to obtain the Lyapunov equation:

$$A^T P + PA = -Q \tag{13}$$

with Q a defined positive symetric matrix. Equation (12) becomes:

$$\dot{V} = -\mathbf{x}^T Q\mathbf{x} + 2\mathbf{x}^T PB(n - \sigma_\theta)$$

To maintain the stability, $\dot{V}$ has to be negative. The first term is negative and the second one is null if $\mathbf{x}$ belongs to the kernel of $B^T P$. We define the sliding variable $s = B^T P\mathbf{x}$. $s = 0$ is the sliding surface. If $s = 0$, the error state vector $\mathbf{x}$ becomes null.

The sliding mode controller σ_θ is defined as $\sigma_\theta(s = 0) = 0$ and for $s \neq 0$, $\sigma_\theta = \mu\frac{s}{\|s\|}$, with μ a positive scalar large enough to allow the stability of the controller. That allows to have:

$$s^T(n - \sigma_\theta) = sn - \mu\frac{s^2}{\|s\|} = sn - \mu\|s\| \leq \|s\|(\|n\| - \mu)$$

If we assume the model error is bounded: $\|n\| \leq n_{Max} < \infty$, the selection of $\mu > n_{Max}$ allows to verify the Lyapunov theorem hypothesis.

4) Solution of the Lyapunov equation: To solve the equation (13), the matrix Q is choosen as:

$$Q = \begin{pmatrix} a & 0 \\ 0 & b \end{pmatrix}$$

with $a > 0$ and $b > 0$.
Knowing the value of the parameters of the matrix A, the matrix P is:

$$P = \begin{pmatrix} \frac{1{,}05\cdot b}{\xi^2\cdot T_r} + \frac{5\cdot a\cdot\xi^2\cdot T_r}{21} + \frac{a\cdot T_r}{16{,}8} & \frac{a\cdot\xi^2\cdot {T_r}^2}{35{,}28} \\ \frac{a\cdot\xi^2\cdot {T_r}^2}{35{,}28} & \frac{b\cdot T_r}{16{,}8} + \frac{a\cdot\xi^2\cdot {T_r}^3}{296{,}352} \end{pmatrix} \tag{14}$$

B. Control of the longitudinal velocity u

Introducing the input τ_u, equations (2) and (5) give us:

$$\dot{u} = \gamma\tau_u + \Lambda_u \sum\dot{\omega} + rv \tag{15}$$

with: $\begin{array}{lcl} \gamma & = & 6/RM \ ; \\ \sum\dot{\omega} & = & \dot{\omega}_{fl} + \dot{\omega}_{fr} + \dot{\omega}_{ml} + \dot{\omega}_{mr} + \dot{\omega}_{rl} + \dot{\omega}_{rr} \ ; \\ \Lambda_u & = & -J_\omega/RM. \end{array}$

As previously, c_u is the control law and $m(u,\dot{u})$ the function of uncertainties depending on u and $\dot{u}$ in the dynamic equations. We have the following relationship:

$$\dot{u} = c_u - m(u,\dot{u}) \tag{16}$$

The longitudinal velocity control law is:

$$c_u = \dot{u}_d + K_p^u \varepsilon_u + \sigma_u \tag{17}$$

with:

- $\dot{u}_d$ an anticipative term;
- $\varepsilon_u = u_d - u$ the velocity error;
- K_p^u a positive constant that permits to define the settling time of the closed-loop system;
- σ_u the sliding mode control law.

Using the Lyapunov candidat function $V = \frac{1}{2}\varepsilon_u^2$, it can be immediately verified that the stability of the system is guaranteed by the choice of the sliding mode control law $\sigma_u = \rho \frac{\varepsilon_u}{\|\varepsilon_u\|}$, with ρ a positive scalar, large enough.

C. Expression of the global control

In practice, uncertainties about the dynamic of the system to control have for consequence an unknown about the real sliding surface $s = 0$. As a consequence $s \neq 0$ and the sliding control law σ, which has a behavior similar to a sign function, induces oscillations while trying to reach the sliding surface $s = 0$ with a null time in theory. These high frequency oscillations around the sliding surface, called chattering, increase the energy consumption and can damage the actuators. In order to reduce them, we can replace the sign function by an *arctan* one or, as chosen here, by adding a parameter with a small value β in the denominator.

Finally, the following torques are applied to each one of the six wheels:

$$\begin{array}{l} \tau_{fl} = \tau_{ml} = \tau_{rl} = \tau_u - \frac{\tau_\theta}{2} \\ \tau_{fr} = \tau_{mr} = \tau_{rr} = \tau_u + \frac{\tau_\theta}{2} \end{array} ; \tag{18}$$

with τ_u and τ_θ defined by:

$$\tau_u = \frac{1}{\gamma}\left(\dot{u}_d + K_p^u \varepsilon_u + \rho \frac{\varepsilon_u}{\|\varepsilon_u\| + \beta_u} - \Lambda_u \dot{\omega} - rv\right) \tag{19}$$

$$\tau_\theta = \frac{1}{\lambda}\left(\dot{\tilde{r}}_d + K_p^\theta \varepsilon_\theta + K_d^\theta \dot{\varepsilon}_\theta + \mu \frac{B^T P \mathbf{x}}{\|B^T P \mathbf{x}\| + \beta_\theta} - \Lambda_\theta \dot{\omega} - \mathbf{D}_\theta \mathbf{F}_\mathbf{y}\right) \tag{20}$$

To estimate the value of the lateral forces $\mathbf{F}_y$, a Pacejka [15] theory could be used by taking into account the slip angle. But, because of the robustness of the sliding mode control, we can consider that $\mathbf{F}_y$ is a perturbation to be rejected, and we do not include it in the control law. A slip angle measure being in practice not very efficient, this solution is better.

IV. USING ROBUBOX TO IMPLEMENT THE CONTROLLER

The sliding mode controller is implemented with Robosoft robuBOX [16], a software package that allows re-usable development and deployment of robotic applications. It is built on top of Microsoft Robotics Studio (MSRS) and is provided by all Robosoft robots. The robuBOX software can also be used without any hardware platform, it runs indifferently on real robotic platforms or in realistic simulations. Using reference designs of architectures provided with robuBOX, the controller algorithm is easily encoded and tuned. Then, we can re-use any existing service within a new architecture.

During the simulation, the RobuROC6 robot is provided with 3D models including the graphic 3D meshes and the physics and dynamics properties. Every joint of this multi-body mobile robot is properly encoded.

Fig. 4. Graphic model of the RobuROC6

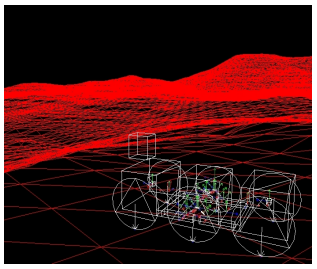

Fig. 5. Physical model of the RobuROC6

Complex environments using a height field entity for the ground are also simulated.

V. SIMULATION

The simulation is executed with RobuBOX, using MSRS and Ageia PhysX [7], a highly realistic 3-dimensional dynamic environment. An advanced tire slip based friction model is used in this simulator. It separates the overall friction force into longitudinal and lateral components. Each component is represented by the function depicted Fig.6, the force being in N and the composite slip, taking into account the longitudinal slip of the tire and the slip angle, without unity. A stiffness factor is also added. This positive gain is the base amount of "grip" of the tire in the specified direction (longitudinal or lateral) [14].

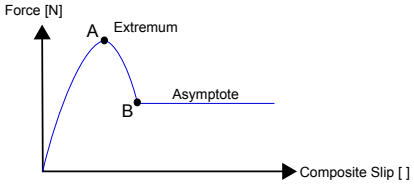

Fig. 6. Friction Model

We use here the following parameters:

- Coordinates of the Extremum point A: $(1.0; 0.02)$;
- Coordinates of the point B, beginning of the Asymptote: $(2.0; 0.01)$;
- Longitudinal stiffness factor $= 10000.0$;
- Lateral stiffness factor $= 10000.0$.

The controller parameters are chosen as: $K_p^u = 1.00\text{s}^{-1}$, $K_p^\theta = 12.00\text{s}^{-2}$, $K_d^\theta = 0.10\text{s}^{-1}$, $\xi = 0.70$, $T_r = 2\text{s}$, $\beta_u = 0.01\text{ms}^{-1}$, $\beta_\theta = 0.01$, $a = 0.10$ and $b = 0.10$ (a and b being the two positive constants defining the matrix Q, solution of the Lyapunov equation). The value of the torques applied on the axis of the wheels are figured with the control law designed in section III.

TABLE I

ROBOT PARAMETERS

Description	Symbol	Value
Length	l	$1.5m$
Width	w	$0.80m$
Height	h	$0.474m$
Mass	M	$140Kg$
Inertia	J	$188Kg \cdot m^2$
Radius of the wheels	R	$0.234m$
Mass of the wheels	M_w	$3Kg$
Inertia of the wheels (also including the inertia of the geared motors)	J_w	$0.364Kg \cdot m^2$

A. *Path following with a horizontal ground*

The first simulation consists of following a curved path on a horizontal ground. In this test, the vehicle is commanded to travel at 3m.s^{-1}. The sliding mode control law gains are so settled: $\rho = 1.0\text{ms}^{-2}$ and $\mu = 18.00$. The displacements of the RobuROC6 are displayed Fig.7. Time evolution of the exerted torques τ_u and τ_θ are displayed Fig.8 and Fig.9 and the evolutions of resulting ε_θ and ε_u with the sliding mode controller are displayed Fig.11 and Fig.10. With a kinematic controller, the vehicle has some difficulties to join the desired path because of the sliding phenomenon in the wheel-soil interaction, not taken into account.
As a consequence, the skidding robot joins the path slowly after a curve.

After adding the sliding mode controller, the robot goes along the path adequately, the torques being continuously corrected. Nevertheless, we can see Fig.11 some oscillations in the yaw angle error plot, what is the chattering phenomenon which can also be seen Fig.10. To reduce steady state error, we can increase the value of the sliding mode controller gains, which increases the value of the robust control input term. But, increasing these gains, the chattering phenomenon increases and the process could present non acceptable vibrations. The best behavior with a good following of the path and with acceptable chattering is plotted for the values reported here. A maximal yaw angle error absolute value of 0.2rad when turning and the longitudinal speed error absolute value always less than 0.4ms^{-1} remain quite satisfactory. Notice that this controller is quite robust because the friction is not constant and some phenomena (e.g. the elasticity of the tire) are not taken into account.

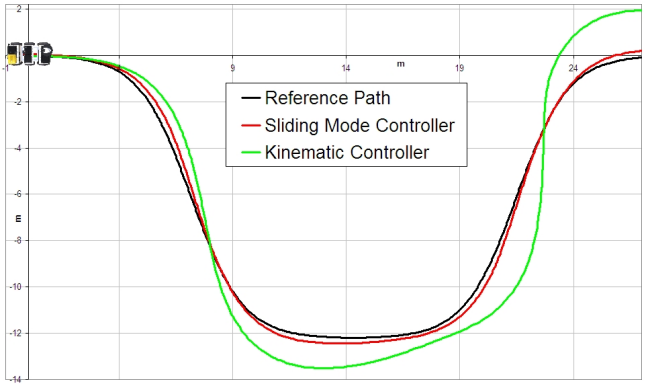

Fig. 7. Robot Position

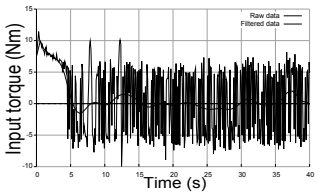

Fig. 8. Torque τ_u

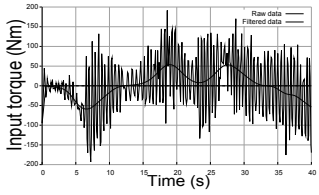

Fig. 9. Torque τ_θ

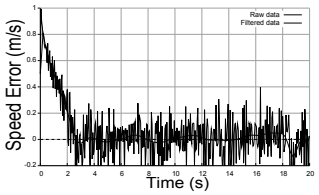

Fig. 10. Longitudinal Speed Error

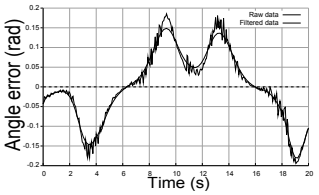

Fig. 11. Yaw Angle Error

B. *Path following with a sinusoidal ground*

In this simulation, we suggest to follow the same path as previously with the same velocity, but with a not horizontal ground in order to investigate the robustness of our controller according to this kind of disturbance. The selected ground has a sinusoidal shape with an amplitude of 0.2m, a little less than the half of the RobuROC6 height, and a period of 2m, a bit longer than its length, as it can be seen Fig.12.

As a result, the path is approximately followed as properly as before. The difference between the position errors of the two simulations, with and without horizontal ground, is plotted Fig.13.

We can see that the curve of the position error with a sinusoidal terrain reaches higher values, due to the added disturbances. But the fluctuations are not significant compared to the vehicle dimensions. So, the controller shows the

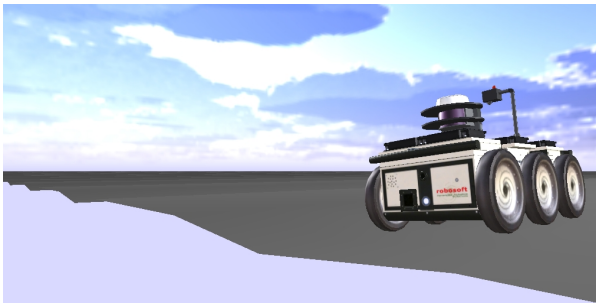

Fig. 12. RobuROC6 on a sinusoidal ground

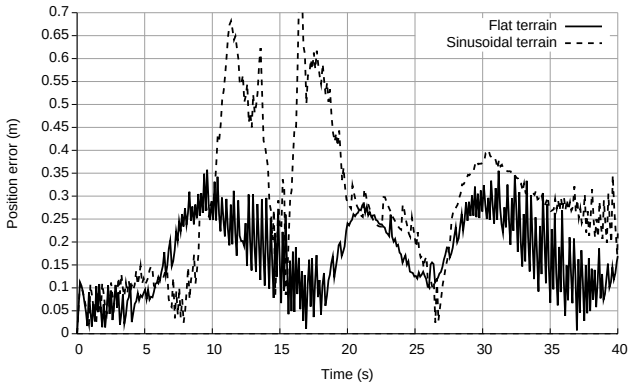

Fig. 13. Position errors

same efficiency as previously with a position error increasing when the robot is turning. Finally, we can conclude that the sliding mode controller is a robust one for the RobuROC6 system, that has its capability, even with disturbances due to fluctuations of the level of the ground.

VI. CONCLUSIONS AND FUTURE WORKS

A sliding mode controller was designed and implemented on the simulated RobuROC6 robot. Using RobuBOX and MSRS, it became easy and fast to develop his own control algorithms and include them in an existing re-usable architecture. The simulations performed with an accurate physical engine have shown the robustness of the control law even without any knowledge about the forces in the wheel-soil interaction and with some fluctuations of the ground level. Next, we will experiment this controller in real conditions. To limit the chattering in the control signals, a second order sliding mode controller may be investigated, as it was already done in [10]. Furthermore, it could be tested in an unstructured environment to evaluate the limits of the controller robustness. In this paper, we have not studied the possibility of varying the sliding mode control law gains. So, we will investigate this possibilty, based on stability criteria like the lateral law transfer (LLT), for exemple already used by Bouton in [4].

REFERENCES

[1] www.robosoft.fr.

[2] Luis E. Aguilar, Tarek Hamel, and Philippe Souères. Robust path following control for wheeled robots via sliding mode techniques. In *IROS*, 1997.

[3] E. Bakker, L. Nyborg, and H.B. Pacejka. Tyre modelling for use in vehicle dynamic studies. *Society of Automotive Engineers*, (paper 870421), 1987.

[4] N. Bouton, R. Lenain, B. Thuilot, and J.-C. Fauroux. A rollover indicator based on the prediction of the load transfer in presence of sliding: application to an all terrain vehicle. In *Proceedings of ICRA'07 : IEEE/Int. Conf. on Robotics and Automation*, pages 1158–1163, April 2007.

[5] Luca Caracciolo, Alessandro De Luca, and Stephano Iannitti. Trajectory tracking control of a four-wheel differentially driven mobile robot. In *Proceedings of the IEEE International Conference on Robotics & Automation*, pages 2632–2638, Detroit, Michigan, May 1999.

[6] M.L. Corradini and G. Orlando. Control of mobile robots with uncertainties in the dynamical model: a discrete time sliding mode approach with experimental results. In Elsevier Science Ltd., editor, *Control Engineering Practice*, volume 10, pages 23–34. Pergamon, 2002.

[7] Jeff Craighead, Robin Murphy, Jenny Burke, and Brian Goldiez. A survey of commercial & open source unmanned vehicle simulators. In *Proceedings of ICRA'07 : IEEE/Int. Conf. on Robotics and Automation*, pages 852–857, Roma, Italy, April 2007.

[8] Lhomme-Desages D., Grand C., and J.C. Guinot. Trajectory control of a four-wheel skid-steering vehicle over soft terrain using a physical interaction model. In *Proceedings of ICRA'07 : IEEE/Int. Conf. on Robotics and Automation*, pages 1164 – 1169, Roma, Italy, April 2007.

[9] F. Hamerlain, K. Achour, T. Floquet, and W. Perruquetti. Higher order sliding mode control of wheeled mobile robots in the presence of sliding effects. In *Decision and Control, 2005 and 2005 European Control Conference. CDC-ECC '05. 44th IEEE Conference on*, pages 1959–1963, 12-15 Dec. 2005.

[10] F. Hamerlain, K. Achour, T. Floquet, and W. Perruquetti. Trajectory tracking of a car-like robot using second order sliding mode control. In *Proceedings of ECC'07: European Control Conference*, pages 4932–4936, Kos, Greece, July 2007.

[11] A. Jorge, B. Chacal, and H. Sira-Ramirez. On the sliding mode control of wheeled mobile robots. In *Systems, Man, and Cybernetics, 1994. 'Humans, Information and Technology'., IEEE International Conference on*, volume 2, pages 1938 – 1943, Oct 1994.

[12] K. Kozlowski and D. Pazderski. Modeling and control of a 4-wheel skid-steering mobile robot. *International journal of applied mathematics and computer science*, 14:477–496, 2004.

[13] F. Le Menn, Ph. Bidaud, and F. Ben Amar. Generic differential kinematic modeling of articulated multi-monocycle mobile robots. In *Proceedings of ICRA'06 : IEEE/Int. Conf. on Robotics and Automation*, pages 1505 – 1510, Orlando, Florida, May 2006.

[14] E. Lucet, Ch. Grand, D. Sall, and Ph. Bidaud. Stabilization algorithm for a high speed car-like robot achieving steering maneuver. In *Proceedings of ICRA'08 : IEEE/Int. Conf. on Robotics and Automation*, pages 2540–2545, Pasadena, USA, 19-23 May 2008.

[15] Hans B. Pacejka. *Tyre and vehicle dynamics*. 2002.

[16] D. Sallé, M. Traonmilin, J. Canou, and V. Dupourqué. Using microsoft robotics studio for the design of generic robotics controllers: the robubox software. In *ICRA 2007 Workshop Software Development and Integration in Robotics - "Understanding Robot Software Architectures"*, Roma, Italy, April 2007.

[17] S. S. Sastry. *Nonlinear systems: Analysis, Stability and Control*. Springer Verlag, 1999.

[18] H.T. Szostak, W.R. Allen, and T.J. Rosenthal. Analytical modeling of driver response in crash avoidance maneuvering volume ii: An interactive model for driver/vehicle simulation. Technical report, U.S Department of Transportation Report NHTSA DOT HS-807-271, April 1988.

[19] V. I. Utkin. *Sliding modes in control optimization.Communication and control engineering series*. Springer - Verlag, 1992.

[20] Jung-Min Yang and Jong-Hwan Kim. Sliding mode control for trajectory tracking of nonholonomic wheeled mobile robots. In *IEEE*, 1999.

View publication stats